Article:
Jurėnas, D, Chatterjee, S, Konijnenberg, A et al. (4 more authors) (2017) AtaT blocks translation initiation by N-acetylation of the initiator tRNAfMet. Nature Chemical Biology, 13 (6). pp. 640-646. ISSN 1552-4450

https://doi.org/10.1038/nchembio.2346

AtaT blocks translation initiation by N-acetylation of the initiator tRNA^{fMet}

Dukas Jurėnas[1,2], Sneha Chatterjee[3,4], Albert Konijnenberg[3,4], Frank Sobott[3,4,5], Louis Droogmans[6], Abel Garcia-Pino[7]* and Laurence Van Melderen[1]*

[1]Laboratoire de Génétique et Physiologie Bactérienne, Université Libre de Bruxelles (ULB), Belgique, [2]Department of Biochemistry and Molecular Biology, Vilnius University Joint Life Sciences Center, Lithuania, [3]Biomolecular and Analytical Mass Spectrometry group, Department of Chemistry, University of Antwerp, Belgium, [4]Astbury Centre for Structural Molecular Biology, University of Leeds, Leeds LS2 9JT, United Kingdom, [5]School of Molecular and Cellular Biology, University of Leeds, LS2 9JT, United Kingdom, [6]Laboratoire de Microbiologie, Université Libre de Bruxelles (ULB), Belgique, [7]Laboratoire de Biologie Structurale et Biophysique, Université Libre de Bruxelles (ULB), Belgium

*Corresponding authors:

Abel Garcia-Pino

Université Libre de Bruxelles (ULB)

Laboratoire de Biologie Structurale et Biophysique,

12 Rue des Professeurs Jeneer et Brachet , B-6041 Gosselies, Belgium

Email: agarciap@ulb.ac.be

Laurence Van Melderen

Université Libre de Bruxelles (ULB)

Laboratoire de Génétique et Physiologie Bactérienne

12 rue des Professeurs Jeener et Brachet, B-6041 Gosselies, Belgium

Email: lvmelder@ulb.ac.be

Abstract

Toxin-antitoxin (TA) loci are prevalent in bacterial genomes. They are suggested to play a central role in dormancy and persister state. Under normal growth conditions TA toxins are neutralized by their cognate antitoxins and under stress conditions toxins are freed and inhibit essential cellular processes using a variety of mechanisms. Here we characterize the *ataR-ataT*, a novel TA locus or system from enterohaemorrhagic *Escherichia coli*. We show that the toxin AtaT is a GNAT family enzyme that transfers an acetyl group from acetyl-coenzyme A to the amine group of the methionyl aminoacyl moiety of initiator tRNA. AtaT specifically modifies Met-tRNA^{fMet} but not other aminoacyl-tRNAs including the elongator Met-tRNA^{Met}. We demonstrate that once acetylated, AcMet-tRNA^{fMet} fails to interact with initiation factor-2 resulting in the disruption of the translation initiation complex. This work reveals a new mechanism of translation inhibition and confirms Met-tRNA^{fMet} as a prime target to efficiently block cell growth.

Introduction

Toxin-antitoxin systems (TA) are widespread in bacterial mobile genetic elements and chromosomes [1-3]. They take part in regulation of important processes such as plasmid stabilization and protection against phages [4,5]. Accumulating evidences indicate that TA systems are involved in the switch to a persister state (highly tolerant to antibiotic) and modulate cell growth under stress conditions [4-7].

TA modules are typically classified according to the nature and mode of action of antitoxins [8,9]. These ubiquitous modules typically consist of a toxic protein and its cognate unstable antitoxin preventing toxin activity or synthesis. In type II TA modules, both components are proteins. During normal growth antitoxins form a tight complex

with their cognate toxins that neutralizes their activity. However once the toxins are released, they target essential cellular processes, resulting in transient cell growth arrest.

Type II toxins present a variety of molecular mechanisms to achieve their functions. They target peptidoglycan synthesis [10], replication [11-13] and translation. Toxins from the RelE and MazF families cleave messenger RNAs with little specificity with or without assistance of ribosomes, respectively [14-16]. Toxins from the VapC family are PIN-domain endonucleases that cleave specifically tRNA and rRNA. Enteric VapCs cleave $tRNA^{fMet}$ in the anticodon stem-loop [17] whereas *M. tuberculosis* VapC20 cleaves the Sarcin–Ricin loop of 23S rRNA [18]. HipA inhibits glutamyl-tRNA synthetase by phosphorylation resulting in the inhibition of the production of $Glu\text{-}tRNA^{Glu}$ [19,20] and Doc phosphorylates the elongation factor EF-Tu thereby interfering with the formation of the ternary complex EF-Tu:GTP:aminoacyl-tRNA[21,22].

Here we identify AtaT-AtaR, a novel type II TA operon found in *Escherichia coli* O157:H7 (AtaT-AtaR for Aminoacyl tRNA acetyltransferase Toxin-Repressor). The toxin, AtaT, contains an N-acetyl-transferase GNAT-domain (Gcn5-related N-acetyltransferase). GNAT enzymes modify a myriad of substrates from small molecules such as antibiotics and metabolites to macromolecules [23]. We demonstrate here that AtaT inhibits translation initiation by specifically acetylating the free amine group of methionine charged on the $tRNA^{fMet}$, using acetyl coenzyme A (AcCoA) as acetyl group donor. Acetylation of the initiator $Met\text{-}tRNA^{fMet}$ prevents interaction with IF2 and formation of an initiation complex compatible with translation initiation. This results in the efficient inhibition of protein synthesis and growth arrest.

Results

ataRT is a novel TA system with a putative acetyltransferase toxin

77 The AtaT (Z4832) from *E. coli* O157:H7, predicted to be an acetyltransferase from the
78 GNAT family accompanies AtaR (Z4833) gene that encodes a putative RHH-domain
79 protein (Supplementary Results, Supplementary Fig. 1). The predicted 9.9 kDa AtaR
80 protein is encoded by the *ataR* gene located 6 bp upstream of the *ataT* gene coding for
81 the predicted 19.7 kDa AtaT protein. GNAT domain proteins in similar genetic
82 organization have been demonstrated to act as toxin-antitoxin pairs [24,25]. Based on these
83 observations we hypothesized that this gene pair encoded a TA module.
84 In order to validate this putative operon as a *bona fide* TA module we cloned the ORFs in
85 compatible vectors carrying different inducible promoters and tested their effect on *E.*
86 *coli* DJ624 viability. Expression of the putative GNAT toxin caused cell growth inhibition
87 while co-expression with AtaR, encoding the putative antitoxin restored cell viability
88 (Fig. 1A).
89 Next we asked if AtaR-AtaT is a type II TA system, with the antitoxin AtaR forming a
90 tight complex with the AtaT toxin that results in the neutralization of the AtaT activity.
91 To test this hypothesis we expressed the proteins from the *ataR-ataT* operon with
92 different affinity tags (his-antitoxin-toxin-strepII) and performed a Ni-sepharose affinity
93 chromatography purification. The AtaR and AtaT proteins co-purified (Fig. 1B) and a
94 complex was separated from an excess of antitoxin after size exclusion chromatography
95 (Fig. 1C). Based on analytical gel filtration we hypothesize that two toxins units and two
96 antitoxins units associate to form a complex of 60 kDa (Supplementary Fig. 2). Native
97 mass spectrometry showed that AtaR-AtaT is a heterogeneous mixture of complexes
98 with different toxin:antitoxin ratios (Supplementary Fig. 3). The predominant species
99 observed at low collision energy consisted of AtaT:AtaR at 1:1 and 2:2 ratios. TA
100 complexes with variable stoichiometries are described for other systems [26-29]. This is a

crucial feature in the regulation of transcription of these operons, allowing a link between toxin neutralization and operon repression[30].

Taken together, these data showed that the *ataR-ataT* gene pair encoded a functional type II TA system similar to the recently described TacTA module from *S. typhimurium* that also contains a GNAT-domain toxin [24].

AtaT inhibits translation in the presence of acetyl-CoA

To determine which cellular process AtaT inhibits, we measured the incorporation of radiolabeled precursors for replication, transcription and translation upon toxin expression *in vivo*. The incorporation of [^{35}S]methionine shown in Fig. 2A was severely affected, indicating that AtaT inhibits translation *in vivo*, without interfering with transcription or replication (Supplementary Fig. 4). As mentioned above, AtaT is predicted to be an acetyltransferase, and possesses the conserved GNAT family topology (Supplementary Fig. 5). We therefore reasoned that translation should be functional in an *in vitro* transcription-translation system in the absence of its potential substrate, AcCoA. Indeed, AtaT was produced to a detectable amount in the absence of AcCoA while upon addition of AcCoA, the protein was no longer synthesized (Fig. 2B) showing that AcCoA was essential for catalysis. Addition of AcCoA did not interfere with the *in vitro* production of the AtaT-AtaR complex or the antitoxin AtaR (Fig. 2B). Moreover *in vitro* translation of a reporter protein (GFP-strepII) was tested in different conditions. In the presence of purified AtaT toxin and AcCoA, GFP-strepII was not produced while addition of AtaR antitoxin restored GFP-strepII synthesis (Fig. 2C). To validate the enzymatic activity of AtaT a G108D mutation was introduced in the conserved AcCoA binding pocket consensus sequence (Q/RxxGxG/A) (Supplementary Fig. 5) [31]. The G108D mutation inactivated AtaT both *in vivo* and *in vitro* (Fig.s 1A, 2C lane 4).

Altogether, these data showed that using AcCoA as co-factor, AtaT blocked translation and that the antitoxin AtaR restored translation completely, even in the presence of AcCoA (Fig. 2C). Moreover, these data indicated that the target of AtaT was present in the *in vitro* transcription-translation system.

AtaT acetylates tRNAs

We used isotope labeled [^{14}C]AcCoA to monitor the acetylation reaction catalyzed by AtaT. The product of the *in vitro* translation reaction resolved on SDS-PAGE gels revealed no isotope signal, suggesting that the target was not a protein or the modification was not stable under the SDS-PAGE conditions. Alternatively, we performed a size fractionation of the reaction product. The ^{14}C signal dotted on a nitrocellulose membrane is retained in fractions corresponding to a size between 30 kDa and 50 kDa (Supplementary Fig. 6). This was confirmed by native PAGE electrophoresis of the *in vitro* translation reactions treated with AtaT and [^{14}C]AcCoA (Fig. 3A). The reaction product was stained with either Coomassie blue or ethidium bromide, or exposed to obtain an autoradiography image. Interestingly, the ^{14}C radioactive signal did not match the band pattern from the Coomassie-stained proteins, but matched the bands corresponding to nucleic acids species stained with ethidium bromide (Fig. 3A). Based on this migration pattern it stands to reason that substrates of AtaT are transfer RNAs (tRNAs). To challenge this hypothesis, a purified mixture of tRNAs from *E. coli* was treated with AtaT and [^{14}C]AcCoA and resolved on a native PAGE gel. Autoradiography confirmed that tRNAs were acetylated by AtaT and that AtaR specifically inhibited this reaction but was unable to reverse it (Fig. 3B).

AtaT modifies the aminoacyl moiety of tRNA

tRNAs are extensively modified as part of their post-transcriptional maturation. N4-acetyl-cytidine is the only known acetylated nucleoside of bacterial tRNAs [32]. To test whether AtaT performed a similar type of modification, an *E. coli* tRNA mixture [^{14}C]acetylated by AtaT was subsequently digested with RNAse P1 and the nucleotide products were resolved by 2D thin layer chromatography (TLC) [33]. Intriguingly the radioactive signal did not correspond to the N4-acetyl-cytidine position and the migration pattern was significantly different to that observed from cognate nucleotides (Supplementary Fig. 7). Noteworthy, the aminoacyl moiety at the CCA tail of aa-tRNAs constitutes an alternative acetylation site to the tRNA nucleotides. In order to test this, we removed the amino acid moiety from the tRNA mixture by alkaline treatment, known to disrupt weak ester bonds and de-acylate tRNAs [34] or using $CuSO_4$. The latter treatment is known to uncharge specifically aminoacyl-tRNA and not peptidyl-tRNAs [35]. A purified *E. coli* tRNA mixture was subjected to the aforementioned treatments before and after the acetylation reaction catalyzed by AtaT using [^{14}C]AcCoA as a substrate (Fig. 4). In both cases, no ^{14}C radioactive signal was detected when the aa-tRNA mixture was uncharged prior acetylation, indicating that acetylation occurred only on aminoacylated tRNAs (Fig. 4A, lanes 3 and 5). Moreover the signal was also lost when the aminoacyl moieties were removed from the tRNAs after the acetylation by alkaline treatment. This indicated that acetylation occurred on the aminoacyl moiety of aatRNAs (Fig. 4A, lane 4). By contrast the $CuSO_4$ treatment failed to remove the amino acids from AtaT-acetylated aminoacyl-tRNAs (Fig. 4A, lane 6). This was a strong indication that upon AtaT treatment, the acetylated-aatRNA species no longer resembled translation-compatible aminoacyl-tRNA (sensitive to $CuSO_4$) and were rather closer to species where the amine group is not free but blocked such as in peptidyl-tRNAs. In addition, chemically

175 acetylated aa-tRNAs (by acetic anhydride) treatment were no longer acetylated by AtaT
176 (Fig. 4A, lane 7), confirming that AtaT acetylated aatRNAs at the free amine group.
177
178 **AtaT is specific for the methionine on Met-tRNA^{fMet}**
179 We produced *in vitro* aminoacylated-tRNA species for each amino acid and tested them
180 to identify the target of AtaT (Fig. 4B). We found that AtaT was highly specific to the
181 initiator tRNA^{fMet} charged with methionine (Met-tRNA^{fMet}) (Fig. 4B). Only very weak
182 acetylation was detected for other tRNAs, including the elongator Met-tRNA^{Met} (Fig. 4B).
183 This suggested that AtaT recognized not only the CCA tail of aa-tRNA but was also able
184 to discriminate the aa-tRNA species based on the acceptor stem and the aminoacyl
185 moiety.
186 The treatment with AtaT and [^{14}C]AcCoA of all possible variants of tRNA^{fMet} either *in*
187 *vitro* synthetized or purified from *in vivo* (not aminoacylated, charged with methionine,
188 charged with methionine and formylated, charged with methionine and chemically
189 acetylated) showed that the ^{14}C labeled acetyl group was transferred only to the free
190 amine group of a tRNA^{fMet} charged with methionine (Fig.s 4C, 4D, Supplementary Fig. 8).
191 Mass spectrometry of Met-tRNA^{fMet} before and after acetylation by AtaT confirmed that
192 the treatment with the enzyme resulted in an increase of mass of approximately 40 Da,
193 that corresponds (ed?) to the approximate mass of an acetyl group (Supplementary Fig.
194 9).
195 To directly confirm these results we performed alkaline treatment on AtaT treated Met-
196 tRNA^{fMet}. AtaT- or acetic anhydride- modified methionine (used as reference), removed
197 from tRNA^{fMet} were analyzed by TLC and mass spectrometry. These results showed that
198 after AtaT treatment, the recovered methionine was acetylated (Supplementary Fig. 10)
199 and mass spectrometry showed that the treatment with AtaT resulted in a mass that

matched the approximate mass of acetyl-methionine (Supplementary Fig. 11). In addition no acetyl-methionine was detectable from Met- tRNA^{fMet} not treated with AtaT (Supplementary Fig. 10 and 11).

Acetylation of Met-tRNA^{fMet} precludes translation initiation

The interaction between the initiator tRNA and IF2 is crucial for the correct assembly of the 30S initiation complex (30S-IC). The recent structure of a 70S ribosome in complex with IF2 and fMet-tRNA^{fMet} showed that IF2 recognizes the aminoacyl-moiety of fMet-tRNA^{fMet} [36]. Therefore we hypothesized that acetylation of Met-tRNA^{fMet} could disrupt this interaction and interfere with translation initiation.

To test this we used isothermal titration calorimetry (ITC) to measure the interaction of IF2 with fMet-tRNA^{fMet} and acMet-tRNA^{fMet}. In the absence of the other components of the initiation complex, IF2 bound fMet-tRNA^{fMet} with a Kd of ~1 μM (similar to reported values[37,38]). By contrast the affinity of IF2 for acMet-tRNA^{fMet} was below the detection level (Fig. 5A). We next tested the effects of acetylation of the initiator tRNA on the assembly of 30S-IC. The 30S-IC was reconstituted *in vitro* incubating 30S ribosomes, mRNA, IF1 and IF2 with formylated or acetylated [^{35}S]Met-tRNA^{fMet} and the efficiency of complex formation was measured by the incorporation of [^{35}S]-labelled initiator tRNA. Our results showed that there was 10-fold decrease of 30S-IC formation in the presence of acetylated Met-tRNA^{fMet} (enzymatically with AtaT or chemically with acetic anhydride) compared to formylated Met-tRNA^{fMet} (Fig. 5B). Altogether these data suggested that AtaT acetylation of the initiator tRNA^{fMet} precluded the interaction of acMet-tRNA^{fMet} with IF2 resulting in the inhibition of translation initiation. Furthermore to assess the validity of this model *in vivo*, we characterized the ribosomal fractions from *E. coli* overexpressing *ataT* or *ataT* and *ataR*. Our results showed that the expression of

225 *ataT* led to extensive accumulation of ribosome assembly intermediates in comparison
226 to control or to *ataR* and *ataT* co-expression (Fig.s 5C, D) in strong support of our model.
227
228 **Discussion**
229 Bacterial type II TA modules have been shown to become active under episodes of
230 stress. They are proposed to assist the stress survival machinery based on their ability
231 to modulate key cellular processes and reversibly arrest cell growth [6]. Translation is a
232 preferred target of type II toxins [9]. They hijack translation at almost every step from
233 mRNA, tRNA and rRNA cleavage to inactivation of translation factors [17-19,21,39]. We
234 unravelled the mechanism of toxicity of the novel type II TA toxin AtaT. Here we showed
235 that AtaT inhibited translation by acetylating initiator Met-tRNA^{fMet} at the amine group
236 of the methionine moiety.
237 AtaT belongs to a new class of bacterial N-acetyltransferases from the GNAT family.
238 GNAT enzymes are found in all domains of life [23,40]. These enzymes acetylate a myriad of
239 targets using AcCoA as a donor group. Knowledge on bacterial GNAT enzymes is scarce,
240 best-studied cases being aminoglycoside-N-acetyltransferases and three protein
241 acetyltransferases RimI, RimJ and RimL known to acetylate the N-termini of ribosomal
242 proteins S18, S5 and L12 respectively [23,41,42]. Notably the GNAT enzyme TmcA is
243 implicated in bacterial translation by modifying the anticodon (CUA) wobble base of the
244 elongator tRNA^{Met} to prevent misreading of similar AUA codon [32]. We showed that,
245 unlike TmcA, AtaT recognizes(d?) both the aminoacyl-CCA moiety and the double
246 stranded stem of the initiator tRNA^{fMet} and acetylates(d?) the amino acid moiety, rather
247 than the tRNA itself (Fig. 4b).
248 During the formation of the 30S-IC, IF2 and fMet-tRNAfMet must bind to the 30S subunit
249 to prime the 30S subunit for subunit joining. IF2 recognizes the CCA-fMet end of the

fMet-tRNA^{fMet} *via* its β-barrel C2 domain[36,43] (Fig. 6a-c). The structure of the fMet-tRNA^{fMet} – 70S ribosome complex shows the terminal A-fMet docks in the cavity formed between the β1-β2 and β4-β5 loops (Fig. 6c). Noteworthy the fMet moiety is surrounded by a network of interactions involving the hydrocarbon part of the side chain of R847 and the π-electrons from the F848 ring of IF2. As shown in Fig. 6c the formyl group is in very close proximity to the phenyl group of F848 [36], therefore it is not surprising that when an acetyl group is modeled instead of formyl (Fig. 6d), the additional methyl moiety introduces clashes likely leading to structural rearrangements (Fig. 6d). Considering that the simple addition of a formyl-group to the initiation Met-tRNA^{fMet} strongly enhances affinity and selectivity for IF2 [44], it is to be expected that a disruptive modification such as acetylation would have a catastrophic impact on the assembly of the initiation complex. The latter is particularly relevant since evidence suggests that simultaneous arrival of IF2 and fMet-tRNA^{fMet} to the 30S-IC, may dominate *in vivo* [38]. Moreover, since acMet-tRNA^{fMet} is a dead-end product whereas fMet-tRNA^{fMet} is continuously used, the activity of AtaT will irrevocably lead to translation inhibition by the accumulation of acMet-tRNA^{fMet} (Fig. 6a). Indeed we show(ed?) that AtaT-dependent acetylation of Met-tRNA^{fMet} precludes(ed?) binding to IF2, the formation of 30S-IC *in vitro* and *in vivo* the assembly of 70S ribosomes. Based on these data, we propose(d?) that *in vivo* AtaT efficiently competes with methionyl-tRNA formyltransferase to modify the methionine moiety of Met-tRNA^{fMet}.

In a recent work (published after submission of this manuscript), TacT, a distant homologue GNAT toxin from *S. typhimurium* (24% sequence identity with AtaT), was shown to acetylate multiple elongation tRNAs thereby inhibiting translation at the elongation step [24]. Although the bases of the inhibition and the impact on ternary complex formation require further investigation, this work suggests that TacT has a

broader specificity compared to AtaT, which is highly specific for the initiator Met-tRNA^{fMet}. This constitutes a remarkable functional divergence within this class of acetyltransferase type II toxins: a sub-family of toxins targets translation at the initiation step while another, with relaxed specificity, targets elongation.

This fuzzy or relaxed specificity seems to be a common functional feature within families of type II toxins. The members of the RelE family show different mRNAs cleavage specificities [14] and even the dependence on the ribosome for catalysis varies. Different VapC toxins cleave different tRNAs and even 23S ribosomal RNA [17,18,45]. More strikingly, toxins from the Doc/Fic family show versatile molecular mechanisms and targets. While Doc phosphorylates the translation elongation factor EF-Tu, FicT AMPylates GyrB and ParE that are subunits of DNA-gyrase and Topoisomerase IV respectively [13,21,46]. It should be noted that sequence similarity within toxin families is usually low most likely a contributing factor to the observed broad specificities and activities. However, the selective pressure driving the divergence in specificity remains to be investigated.

In terms of physiological function, the TacTA system was shown to promote persister cells formation in *S. typhimurium* [24]. Further work on the impact of AtaT-dependent translation initiation inhibition in the context of the stress response and persistence will be needed to unravel the biological roles of the *ataRT* system. The work presented here represents a crucial step forward in this challenging endeavour.

Acknowledgements

D.J. is a PhD fellow at FNRS (aspirant FNRS). This work was supported by the Fonds Jean Brachet and the Fondation Van Buuren to L.D., the Fonds National de la Recherche Scientifique (FNRS, grant number: F.4505.16 MIS), the Fonds d'Encouragement à la Recherche ULB (FER-ULB), the Fonds Jean Brachet and the Fondation Van Buuren to

A.G.P., the Fonds National de la Recherche Scientifique (FNRS, grant number: 3.4621.12 FRSM, T.0147.15F PDR and J.0061.16F CDR), the Interuniversity Attraction Poles Program initiated by the Belgian Science Policy Office (MICRODEV), Fonds Jean Brachet and Fondation Van Buuren to L.V.M. Authors would like to thank Javier Mateo Sanz for initial works characterizing the *ataR-ataT* system.

Data availability

All data generated or analyzed during this study are included in this published article (and its supplementary information files) or are available from the corresponding author on reasonable request.

Author Contributions:

D.J., L.D., A.G.P. and L.V.M. designed research; D.J., A.G.P., A.K., and S.C. performed research; D.J., A.K., S.C., F.S., L.D., A.G.P. and L.V.M. analyzed data; and D.J., A.G.P. and L.V.M. wrote the paper.

Conflict of interest:

The authors declare no conflict of interest.

References

1. Leplae, R. et al. Diversity of bacterial type II toxin-antitoxin systems: a comprehensive search and functional analysis of novel families. *Nucleic Acids Res* **39**, 5513-25 (2011).
2. Makarova, K.S., Wolf, Y.I. & Koonin, E.V. Comprehensive comparative-genomic analysis of type 2 toxin-antitoxin systems and related mobile stress response systems in prokaryotes. *Biol Direct* **4**, 19 (2009).

3. Pandey, D.P. & Gerdes, K. Toxin-antitoxin loci are highly abundant in free-living but lost from host-associated prokaryotes. *Nucleic Acids Res* **33**, 966-76 (2005).
4. Magnuson, R.D. Hypothetical functions of toxin-antitoxin systems. *J Bacteriol* **189**, 6089-92 (2007).
5. Van Melderen, L. Toxin-antitoxin systems: why so many, what for? *Curr Opin Microbiol* **13**, 781-5 (2010).
6. Maisonneuve, E. & Gerdes, K. Molecular mechanisms underlying bacterial persisters. *Cell* **157**, 539-48 (2014).
7. Brauner, A., Fridman, O., Gefen, O. & Balaban, N.Q. Distinguishing between resistance, tolerance and persistence to antibiotic treatment. *Nat Rev Microbiol* **14**, 320-30 (2016).
8. Yamaguchi, Y. & Inouye, M. Regulation of growth and death in Escherichia coli by toxin-antitoxin systems. *Nat Rev Microbiol* **9**, 779-90 (2011).
9. Hayes, F. & Van Melderen, L. Toxins-antitoxins: diversity, evolution and function. *Crit Rev Biochem Mol Biol* **46**, 386-408 (2011).
10. Mutschler, H., Gebhardt, M., Shoeman, R.L. & Meinhart, A. A novel mechanism of programmed cell death in bacteria by toxin-antitoxin systems corrupts peptidoglycan synthesis. *PLoS Biol* **9**, e1001033 (2011).
11. Bernard, P. & Couturier, M. Cell killing by the F plasmid CcdB protein involves poisoning of DNA-topoisomerase II complexes. *J Mol Biol* **226**, 735-45 (1992).
12. Jiang, Y., Pogliano, J., Helinski, D.R. & Konieczny, I. ParE toxin encoded by the broad-host-range plasmid RK2 is an inhibitor of Escherichia coli gyrase. *Mol Microbiol* **44**, 971-9 (2002).
13. Harms, A. et al. Adenylylation of Gyrase and Topo IV by FicT Toxins Disrupts Bacterial DNA Topology. *Cell Rep* **12**, 1497-507 (2015).
14. Goeders, N., Dreze, P.L. & Van Melderen, L. Relaxed cleavage specificity within the RelE toxin family. *J Bacteriol* **195**, 2541-9 (2013).
15. Pedersen, K. et al. The bacterial toxin RelE displays codon-specific cleavage of mRNAs in the ribosomal A site. *Cell* **112**, 131-40 (2003).
16. Zhang, Y. et al. MazF cleaves cellular mRNAs specifically at ACA to block protein synthesis in Escherichia coli. *Mol Cell* **12**, 913-23 (2003).

17. Winther, K.S. & Gerdes, K. Enteric virulence associated protein VapC inhibits translation by cleavage of initiator tRNA. *Proc Natl Acad Sci U S A* **108**, 7403-7 (2011).
18. Winther, K.S., Brodersen, D.E., Brown, A.K. & Gerdes, K. VapC20 of Mycobacterium tuberculosis cleaves the Sarcin-Ricin loop of 23S rRNA. *Nat Commun* **4**, 2796 (2013).
19. Germain, E., Castro-Roa, D., Zenkin, N. & Gerdes, K. Molecular mechanism of bacterial persistence by HipA. *Mol Cell* **52**, 248-54 (2013).
20. Kaspy, I. et al. HipA-mediated antibiotic persistence via phosphorylation of the glutamyl-tRNA-synthetase. *Nat Commun* **4**, 3001 (2013).
21. Castro-Roa, D. et al. The Fic protein Doc uses an inverted substrate to phosphorylate and inactivate EF-Tu. *Nat Chem Biol* **9**, 811-7 (2013).
22. Garcia-Pino, A. et al. Doc of prophage P1 is inhibited by its antitoxin partner Phd through fold complementation. *J Biol Chem* **283**, 30821-7 (2008).
23. Vetting, M.W. et al. Structure and functions of the GNAT superfamily of acetyltransferases. *Arch Biochem Biophys* **433**, 212-26 (2005).
24. Cheverton, A.M. et al. A Salmonella Toxin Promotes Persister Formation through Acetylation of tRNA. *Mol Cell* **63**, 86-96 (2016).
25. Iqbal, N., Guerout, A.M., Krin, E., Le Roux, F. & Mazel, D. Comprehensive Functional Analysis of the 18 Vibrio cholerae N16961 Toxin-Antitoxin Systems Substantiates Their Role in Stabilizing the Superintegron. *J Bacteriol* **197**, 2150-9 (2015).
26. Dao-Thi, M.H. et al. Intricate interactions within the ccd plasmid addiction system. *J Biol Chem* **277**, 3733-42 (2002).
27. Overgaard, M., Borch, J., Jorgensen, M.G. & Gerdes, K. Messenger RNA interferase RelE controls relBE transcription by conditional cooperativity. *Mol Microbiol* **69**, 841-57 (2008).
28. Garcia-Pino, A. et al. Allostery and intrinsic disorder mediate transcription regulation by conditional cooperativity. *Cell* **142**, 101-11 (2010).
29. Afif, H., Allali, N., Couturier, M. & Van Melderen, L. The ratio between CcdA and CcdB modulates the transcriptional repression of the ccd poison-antidote system. *Mol Microbiol* **41**, 73-82 (2001).

30. Loris, R. & Garcia-Pino, A. Disorder- and dynamics-based regulatory mechanisms in toxin-antitoxin modules. *Chem Rev* **114**, 6933-47 (2014).
31. Neuwald, A.F. & Landsman, D. GCN5-related histone N-acetyltransferases belong to a diverse superfamily that includes the yeast SPT10 protein. *Trends Biochem Sci* **22**, 154-5 (1997).
32. Ikeuchi, Y., Kitahara, K. & Suzuki, T. The RNA acetyltransferase driven by ATP hydrolysis synthesizes N4-acetylcytidine of tRNA anticodon. *EMBO J* **27**, 2194-203 (2008).
33. Grosjean, H., Keith, G. & Droogmans, L. Detection and quantification of modified nucleotides in RNA using thin-layer chromatography. *Methods Mol Biol* **265**, 357-91 (2004).
34. Schuber, F. & Pinck, M. On the chemical reactivity of aminoacyl-tRNA ester bond. I. Influence of pH and nature of the acyl group on the rate of hydrolysis. *Biochimie* **56**, 383-90 (1974).
35. Janssen, B.D., Diner, E.J. & Hayes, C.S. Analysis of aminoacyl- and peptidyl-tRNAs by gel electrophoresis. *Methods Mol Biol* **905**, 291-309 (2012).
36. Sprink, T. et al. Structures of ribosome-bound initiation factor 2 reveal the mechanism of subunit association. *Sci Adv* **2**, e1501502 (2016).
37. Mitkevich, V.A. et al. Thermodynamic characterization of ppGpp binding to EF-G or IF2 and of initiator tRNA binding to free IF2 in the presence of GDP, GTP, or ppGpp. *J Mol Biol* **402**, 838-46 (2010).
38. Tsai, A. et al. Heterogeneous pathways and timing of factor departure during translation initiation. *Nature* **487**, 390-3 (2012).
39. Neubauer, C. et al. The structural basis for mRNA recognition and cleavage by the ribosome-dependent endonuclease RelE. *Cell* **139**, 1084-95 (2009).
40. Vetting, M.W., Bareich, D.C., Yu, M. & Blanchard, J.S. Crystal structure of RimI from Salmonella typhimurium LT2, the GNAT responsible for N(alpha)-acetylation of ribosomal protein S18. *Protein Sci* **17**, 1781-90 (2008).
41. Tanaka, S., Matsushita, Y., Yoshikawa, A. & Isono, K. Cloning and molecular characterization of the gene rimL which encodes an enzyme acetylating ribosomal protein L12 of Escherichia coli K12. *Mol Gen Genet* **217**, 289-93 (1989).

42. Yoshikawa, A., Isono, S., Sheback, A. & Isono, K. Cloning and nucleotide sequencing of the genes rimI and rimJ which encode enzymes acetylating ribosomal proteins S18 and S5 of Escherichia coli K12. *Mol Gen Genet* **209**, 481-8 (1987).
43. Guenneugues, M. et al. Mapping the fMet-tRNA(f)(Met) binding site of initiation factor IF2. *EMBO J* **19**, 5233-40 (2000).
44. Milon, P. et al. The ribosome-bound initiation factor 2 recruits initiator tRNA to the 30S initiation complex. *EMBO Rep* **11**, 312-6 (2010).
45. Winther, K., Tree, J.J., Tollervey, D. & Gerdes, K. VapCs of Mycobacterium tuberculosis cleave RNAs essential for translation. *Nucleic Acids Res* (2016).
46. Garcia-Pino, A., Zenkin, N. & Loris, R. The many faces of Fic: structural and functional aspects of Fic enzymes. *Trends Biochem Sci* **39**, 121-9 (2014).

Fig. legends

Fig. 1: The *ataT-ataR* genes pair constitutes a type II TA system. (a) Overnight cultures of *E. coli* strains transformed with pBAD33 and pKK223-3 vectors or derivatives expressing the *ataT* gene, the *ataT* G108D mutant, the *ataR* gene or the *ataT* and *ataR* genes were serially diluted (-1 to -8). Dilutions were spotted on LB medium supplemented with appropriate antibiotics and 0.2 % glucose (repression conditions, left panel) and 0.2% arabinose and 1 mM IPTG (induction conditions, right panel). (b) Ni-affinity purification of his-AtaR-AtaT-strepII complex. Elution fractions were resolved by SDS-PAGE and stained with Coomassie blue. Lanes 1 to 6: fractions corresponding to 0, 20, 50, 80, 150 and 500 mM imidazole, respectively. (c) Fraction 6 subjected to size exclusion chromatography resulted in two peaks corresponding to his-AtaR-AtaT-strepII complex and his-AtaR antitoxin as seen on SDS-PAGE and stained with Coomassie blue (lanes 1 and 2) and anti-his (lanes 3 and 4) or anti-strepII (lanes 5 and 6) western blots. M: molecular weight marker. Images of all of the full gels are shown in **Supplementary Fig. 12.**

Fig. 2: AtaT inhibits translation in an AcCoA-dependent manner. (a) *In vivo* translation rate measured by incorporation of [^{35}S]methionine after 1 hour of expression of *ataT, yoeB* or *parE2* (type II toxins inhibiting translation and replication, respectively) as controls. Translation rate in the different strains is normalized to that containing the pBAD33 vector. Error bars indicate standard deviation of three independent experiments. (b) Synthesis of AtaT, AtaR or both proteins expressed from T7 promoter in the *in vitro* transcription-translation system supplemented with [^{35}S]methionine. Reactions were carried out with AcCoA (lanes 2, 5 and 7) or without AcCoA (lanes 1, 4 and 6). Lane 3 is a control without [^{35}S]methionine. Samples were resolved by SDS-PAGE and exposed to phosphor storage screen. (c) Synthesis of GFP-strepII reporter protein expressed from T7 promoter in the *in vitro* transcription-translation system. Products of translation reactions were resolved by SDS-PAGE followed by western blot with anti-strepII tag antibodies. "Mut" indicates the use of the AtaT G108D mutant. Images of the full gels are shown in **Supplementary Fig. 12.**

Fig. 3: AtaT acetylates tRNAs. (a) Acetylation reaction in the *in vitro* transcription-translation system supplemented with [^{14}C]AcCoA. Reaction products resolved by native PAGE in three replicas and stained with Coomassie blue (lanes 1-3) or with ethidium bromide (lanes 4-6). Gel comprising lanes 7-9 was dried and exposed to phosphor storage screen. (b) *In vitro* acetylation reactions of tRNA mixture purified from *E. coli* supplemented with [^{14}C]AcCoA. Reaction products were resolved by native PAGE, stained with methylene blue (upper panel) and exposed to phosphor storage screen (lower panel). Lane 1: control tRNAs with [^{14}C]AcCoA, lane 2: control tRNAs with AtaT toxin, lane 3: tRNAs with AtaT and [^{14}C]AcCoA, lane 4: AtaR was premixed with AtaT

before acetylation reaction, Lane 5: AtaR was added after acetylation reaction (indicated by *). The reaction was then allowed to continue for 30 min. Images of the full gels are shown in **Supplementary Fig. 12.**

Fig. 4: AtaT acetylates the amine group of the methionine charged on the initiator tRNA. (a) *In vitro* acetylation reactions of aminoacyl moiety of *E. coli* tRNA mixture supplemented with [^{14}C]AcCoA. Products were resolved by native PAGE, stained with methylene blue (upper panel) and exposed to phosphor storage screen (lower panel). Lane 1: control, lane 2: addition of AtaT, lane 3: alkaline treatment of tRNA mixture using Tris-HCl pH 9.5 before acetylation, lane 4: same treatment after acetylation, lane 5: $CuSO_4$ treatment of tRNA mixture before acetylation, lane 6: same treatment after acetylation, lane 7: acetic anhydride treatment of tRNA mixture before acetylation. (b) AtaT acetylation reactions with individual aa-tRNA species using [^{14}C]AcCoA. Products were resolved by native PAGE, stained with methylene blue (upper panel) and exposed to phosphor storage screen (lower panel). Lane 1: Charged initiator tRNA (Met-tRNA^{fMet}). Lane 2-21: tRNAs charged with their respective amino acids. tRNA species are indicated in online methods. (c) Acetylation of synthetic tRNA^{fMet} species with [^{14}C]AcCoA and with AtaT or without AtaT (controls). Reaction products were resolved by native PAGE, stained with methylene blue (upper panel) and exposed to phosphor storage screen (lower panel). Reactions were carried out using uncharged tRNA^{fMet} (lanes 1, 2), tRNA^{fMet} charged with methionine (lanes 3, 4), tRNA^{fMet} charged with methionine and formylated (lanes 5, 6), tRNA^{fMet} charged with methionine and chemically N-acetylated (lanes 7, 8). (d) Representation of initiator tRNA^{fMet}. The arrow indicates the amine group modified by AtaT. Images of the full gels are shown in **Supplementary Fig. 12.**

Fig. 5: Translation initiation inhibition *in vitro* and *in vivo* by AtaT. (a) Interaction of IF2 with fMet-tRNA^{fMet} (left panel), and acMet-tRNA^{fMet} (right panel) monitored by ITC. (b) *In vitro* formation of 30S-IC using 30S ribosomes, IF1, IF2, mRNA and tRNA^{fMet} charged with [^{35}S]-Met and modified as indicated on the X axis. The complex formation was allowed for 10 min, protein complexes were trapped on nitrocellulose filters and incorporation of isotope labelled tRNA^{fMet} was measured in scintillation counter (the data represents mean values ± s.d, each measurement was repeated at least three times) (c) Ribosome profiles. Cultures of *E. coli* strains transformed with pBAD33 and pKK223-3 vectors (black curve) or derivatives expressing the *ataT* gene (red curve) or the *ataT* and *ataR* genes (blue curve) were grown to an $OD_{600\ nm}$ of 0.2. Arabinose was added at 0.2% for 1 hour and cultures were treated with 0.5 mg/ml of chloramphenicol for 3 min. Cell extracts were centrifuged on sucrose gradient, fractions were collected top-down and $OD_{260\ nm}$ was measured. The fractions that were used for rRNA extraction are indicated with a star (d) to confirm identity of the peaks 1-4 (left to right). rRNA was analysed by agarose gel electrophoresis followed by staining with ethidium bromide. Images of the full gels are shown in **Supplementary Fig. 12.**

Fig. 6:

Proposed mode of action of AtaT. (a) Scheme of translation initiation in bacteria. During this step of translation, the initiation factors IF1, IF2 and IF3 are tasked with ribosome subunit dissociation and anti-association, the selection of the initiator aa-tRNA, the selection of the correct translation start site, and the subunit joining at the start codon. AtaT (labeled in red) interferes with the initiation process by acetylating the initiator Met-tRNA^{fMet}. (b) Cryo electron microscopy structure of fMet-tRNA^{fMet} and IF2

524 bound to the *E. coli* ribosome (PDBID 3JCJ [36]). The 50S and 30S subunits are colored in
525 blue, IF_2 is shown in green and fMet-$tRNA^{fMet}$ in magenta. The A-formyl-Met end is
526 recognized by the C2 β–barrel domain of IF2. (c) Detailed view on the interaction
527 between IF_2 and fMet-$tRNA^{fMet}$ at the CCA end. The aliphatic side chains of R847 and
528 E860 together with the aromatic ring of F848 enclose the formyl-Methionine. Notably
529 the phenyl-group of F848 is in close contact with the formyl- group. (d) If an acetyl
530 group is modeled on the amine moiety of the Methionine the distances between the
531 extra methyl group and the ring of F848 become less than 1.5Å (black circle).
532

Online Methods

Media and general growth conditions

Killing-rescue assays were performed on solid LB (Lennox L broth, Invitrogen) medium. *In vivo* translation, transcription and replication assays were performed in liquid M9 medium (KH_2PO_4 (22 mM), Na_2HPO_4 (42 mM), NH_4Cl (19 mM), $MgSO_4$ (1 mM), $CaCl_2$ (0.1 mM), NaCl (9 mM)) supplemented with 0.2 % casamino acids (0.05 % in the case of [^{35}S]-methionine incorporation). Repression medium was supplemented with 1% glucose prior to induction. At the time of induction, cultures were centrifuged and pellets were washed and resuspended in medium with glycerol (1%) as carbon source. Antibiotic concentrations were as follows – chloramphenicol 20 µg/ml, ampicillin 100 µg/ml. Strains used in this work are listed in Supplementary table 1.

Bioinformatic identification of AtaR-AtaT TA system

We have developed a bioinformatics approach to identify novel TA systems (J. Guglielmini and L. Van Melderen, unpublished). The prediction criteria are based on the canonical genetic organisation of type II TAs assuming that they are generally composed of 2 small ORFs, organized in an operon with small intergenic or overlapping region. Using this approach, we identified the Z4832-Z4833 gene pair located in the chromosome of *E. coli* O157:H7. The two ORFs located in an operon consist of small ribbon-helix-helix (RHH)-domain transcription regulator (88 amino acid residues) and GNAT-family acetyltransferase of moderate size (175 amino acid residues).

Plasmid constructions

Oligonucleotides were synthesized by Sigma-Aldrich and their sequences are listed in Supplementary table 2. Genes for cloning were amplified by PCR using Q5 polymerase

(NEB), purified with GenElute PCR Cleanup kit (Sigma-Aldrich), digested with restriction enzymes (NEB) and ligated with T4 ligase (NEB) with vectors digested with appropriate restriction enzymes. Ligation mixes were transformed by electroporation in *E. coli* DJ624Δ*ara*. The *ataT* gene was amplified with *ataT-for-XbaI* and *ataT-rev-PstI* primers and cloned in pBAD33 vector. The *ataR* gene was amplified with *ataR-for-EcoRI* and *ataR-rev-PstI* primers and cloned in pKK223-3 vector. The *his-ataR-ataT-strepII* operon was amplified using *ataR-for-his-EcoRI* and *ataT-rev-strepII-PstI* primers and cloned in pKK223-3 vector. Mutatation in pBAD33-AtaT was introduced by amplifying plasmid with phosphorylated primers *ataT-revM-G108D* and *ataT-for-G108D* and circularizing the vector with T4 ligase. Sequences of all the constructs were confirmed by sequencing (Cogenics/Genewiz).

Killing-rescue assay

E. coli DJ624Δ*ara* strains were transformed with compatible pBAD33 and pKK223-3 vectors encoding toxin and antitoxin respectively or control vectors. Overnight cultures in LB medium supplemented with appropriate antibiotics and 1% glucose were diluted serially (10-fold) and 10 µl of dilutions were spotted on solid LB plates supplied with antibiotics and 0.2 % glucose (repression conditions) or 0.2% arabinose and 1 mM IPTG (isopropyl β-D-1-thiogalactopyranoside) (induction conditions). Plates were incubated overnight at 37 °C.

***In vivo* translation, transcription and replication assays**

E. coli DJ624Δ*ara* strain was transformed with pBAD33 vector and derivatives containing the *ataT* gene and *yoeB* or *parE2* genes as controls. Strains were grown in M9 minimal medium and arabinose (0.2 %) was added at an OD_{600nm} of 0.3. Translation

583 rates were estimated by measuring incorporation of L-[^{35}S]-methionine (PerkinElmer).
584 One hour after induction, 1 ml of culture was incubated with 3 µCi of [^{35}S]-methionine
585 for 5 min. Samples were then precipitated with 5 ml of 10% TCA for 30 minutes at 4°C
586 and macromolecules were trapped on 0.45µm nitrocellulose filters. Filters were washed
587 with 20 ml of 10% TCA, air dried and immersed in 10 ml of scintillation liquid
588 (Optiphase Hisafe 2, PerkinElmer). Counts per minute from filter-trapped
589 macromolecules were detected in liquid scintillation counter (Beckman). *In vivo*
590 transcription and replication were followed using the same protocol, except that
591 cultures were incubated with [^{3}H]-uridine (1 µCi/ml) or [^{3}H]-thymidine (1 µCi/ml)
592 (PerkinElmer), respectively.
593
594 ***In vitro* translation assays**
595 *In vitro* translation assays were performed using PURExpress™ (NEB) coupled
596 transcription-translation system. Reactions were supplied with 250 ng of DNA
597 fragments containing T7 promoter and genes of interest obtained by PCR using primers
598 listed in Supplementary table 2. Protein synthesis was estimated by performing
599 reactions in the presence of 1 µM of [^{35}S]-methionine. Reaction products were resolved
600 on a 4-20% SDS-PAGE gel (BioRad), which was then dried and exposed to multipurpose
601 phosphor storage screen (Amersham) overnight and scanned using Storm 860
602 PhosphoImager system (Molecular dynamics). Translation of the reporter protein (GFP-
603 strepII) was followed by Western Blot using antibodies against strepII affinity tag.
604
605 **Proteins production and purification**
606 His-AtaR/AtaT-strepII complex and free AtaR antitoxin were purified using ÄKTA
607 Explorer FPLC purifier (GE-Healthcare). *E. coli* DJ624Δ*ara* strain containing the pKK223-

3-his-*ataR-ataT*-strepII plasmid was grown in LB medium to an OD_{600nm} of 0.7. Expression of the proteins of interest was induced by adding 0.5 mM IPTG, and cells were grown overnight at 30°C. The culture was then centrifuged and pellet was resuspended in resuspension buffer (50 mM Tris-HCl pH 8.5, 500 mM NaCl, 2 mM imidazole, 1 mM TCEP). Cells were disrupted using high pressure homogenizer (Microfluidics), lysate was centrifuged at 18,000 rpm for 30 min and filtered through a 0.45µm filter to remove cell debris. Protein extract was loaded on HisTrapHP column (GE Healthcare), washed with buffer A (50 mM Tris-HCl pH 8.5, 500 mM NaCl) and eluted with gradient of buffer B (25 mM Tris-HCl pH 8.5, 250 mM NaCl, 1M imidazole). AtaT-AtaR complex and excess of free AtaR antitoxin were separated by gel filtration on HiLoad Superdex 75 PG column (GE Healthcare). Gel filtration was performed in buffer A. Expression of formyl-methionyltransferase (FMT) and initiation factors IF1 and IF2 were induced with IPTG (0.5 mM) and purified from ASKA collection vectors[47] by histidine affinity chromatography, followed by gel filtration in the same manner as described above.

AtaT-strepII toxin was produced *in vitro* with PURExpress™ (NEB) coupled transcription-translation system and purified using Strep-Tactin Sepharose (IBA). T7-*ataT*-strepII DNA fragment was amplified by PCR from *E. coli* O157:H7 EDL933 chromosome using primers *5'UTR-ataT* and *3'UTR-ataT-strepII* (table S2). The PCR product was purified by phenol-chloroform extraction and ethanol precipitation. 250 µl of transcription-translation reaction was supplied with 2.5 µg of T7-*ataT*-strepII DNA template and incubated for 4 hours at 37 °C. Reaction was then diluted 3 times with binding buffer (100 mM Tris-HCl pH 8.5, 150 mM NaCl, 1 mM EDTA) and loaded on 200 µl of Strep-Tactin Sepharose. Column was washed with 10 column volumes of binding buffer and protein was eluted with 200 µl of elution buffer (binding buffer with 10 mM

633 desthiobiotin). The eluted protein was then purified on PD SpinTrap G-25 column (GE
634 Healthcare), aliquoted and stored at -20°C.
635
636 **Total *E. coli* tRNA purification**
637 Total *E. coli* tRNA was extracted from *E. coli* XL1-Blue cells as described in [48].
638
639 **tRNA synthesis and aminoacylation**
640 tRNA transcripts were synthesized in vitro using MEGAscript T7 transcription kit
641 (Thermo Fisher Scientific) from synthetic dsDNA oligonucloetides (Sigma-Aldrich) listed
642 in Supplementary table 2. When needed the first nucleotide was changed to G to
643 increase synthesis ($tRNA^{fMet}$, $tRNA^{Ile}$, $tRNA^{Trp}$, $tRNA^{Pro}$, $tRNA^{Asn}$, $tRNA^{Gln}$) and accordingly
644 nucleotide preceding ACCA at 3' terminus was changed to C to obtain base pairing and
645 stabilize the tRNAs. Sense and antisense oligonucleotides were mixed together, heated
646 at 95°C for 5 min and allowed to cool down at room temperature. T7 transcription
647 reactions were performed according to manufacturer recommendations. *In vivo* $tRNA^{fMet}$
648 containing all modifications was purchased from tRNA Probes. tRNAs were charged
649 using *E. coli* S100 fraction as described in [49]. Charging was confirmed by using [^{35}S]-
650 methionine as substrate for $tRNA^{Met}$ and $tRNA^{fMet}$, as well as some [^{14}C] amino acids for
651 their respectful tRNAs (Val, Ile). Formylation of Met-$tRNA^{fMet}$ was performed as
652 described in [49] using purified formyl-methionyltransferase protein. tRNAs were phenol-
653 chloroform purified, precipitated in ethanol and dissolved in water.
654
655 **Acetylation assays**
656 Ten µg of purified *E. coli* tRNA mixture or 2 µg of a single tRNA species were used for
657 acetylation reactions. Reactions were performed using 0.2 µM of AtaT-strepII toxin with

or without 2 μM of AtaR antitoxin. Reactions were supplied either with 100 μM cold or radiolabeled [^{14}C]Ac-CoA (60 mCi/mmol). Reactions were incubated at 37 °C for 30 minutes. tRNAs were resolved on 10% native acrylamide (19:1) TBE (Tris-borate EDTA) gels. Gels were stained with 0.2 % methylene blue solution. Stained gels were photographed and then dried and exposed for 12 to 36 hours to multipurpose phosphor storage screen (Amersham) and scanned with Storm 860 PhosphoImager system (Molecular dynamics). Acetylation assays in translation reactions were performed by supplementing the reactions with AtaT, AtaR and [^{14}C]-AcCoA as described above.

tRNA deacylation and chemical acetylation

Unfractionated tRNA mixture or single tRNA species were deacetylated by incubation in 0.1M Tris-HCl pH 9.5 at 37 °C for 1h. tRNAs were also deacylated using copper(II) sulphate as described in [35]. Charged tRNAs were chemically N-acetylated using acetic anhydride as described in [50]. After treatments tRNAs were dialysed against water or precipitated and dissolved in water.

Thin layer chromatography

For nucleotide 2D thin layer chromatography 20 μg of unfractionated tRNA mixture was acetylated with toxin using [^{14}C]-Acetyl-CoA in 20 μl reaction as described above. After acetylation reaction, tRNAs were purified by phenol-chloroform extraction and ethanol precipitation. Reaction was digested with 2U of nuclease P1 (Sigma-Aldrich) overnight at 37 °C and spotted on cellulose TLC plate (Millipore). First dimension was resolved in isobutyric acid/ammonia/water (66/1/33). Second dimension was resolved either in phosphate buffer pH6.8/NH4 sulfate/n-propanol (100/60/2) (Solvent system 1) or in isopropanol/HCl/water (68/18/14) (Solvent system 2). Positions of canonical

683 nucleotides were determined under UV light and plates were exposed to multipurpose
684 phosphor screen (Amersham) scanned with Storm 860 PhosphoImager system
685 (Molecular dynamics).
686 For amino acid thin layer chromatography [^{35}S]Methionine from tRNA^{fMet} were
687 uncharged using ammonia and resolved on silica gel plates in butanol/water/acetic acid
688 (4/1/1) as previously described[50].
689
690 **Mass spectrometry**
691 Samples of the AtaT-AtaR were prepared at 20 µM of complex in 100 mM ammonium
692 acetate buffer, pH 6.9. The treated and non-treated Met-tRNA^{fMet} samples prepared at 10
693 µM were also prepared in 100 mM ammonium acetate buffer, pH 6.9. All the samples
694 were introduced into the mass spectrometer using nanoelectrospray ionization with in-
695 house-prepared gold-coated borosilicate glass capillaries with a voltage of
696 approximately +1.6 kV. Spectra were recorded on a Synapt G2 Q-TOF in TOF mode
697 modified for transmission of native, high m/z protein assemblies as described
698 previously [51] or on a Synapt G2 Q-TOF (Waters, Manchester, UK) in TOF-mode.
699 The separation of the amino-acyl charge of treated and non-treated Met-tRNA^{fMet} was
700 performed using hydrophilic interaction liquid chromatography (*HILIC*) on a Waters
701 Acquity UPLC instrument equipped with an Acquity BEH amide column using 0,1%
702 formic acid in H_2O as solvent A and 0,1% formic acid in acetonitrile as solvent B. The
703 gradient was run from 7% to 80% A over the course of 8 minutes. Standards for both
704 methionine and acetylated methionine were observed at around 3.36 minutes and 3.45
705 minutes respectively. We used Multiple-Reaction Monitoring (MRM) to detect the
706 presence of acetylated methionine. In a MRM experiment the parent of the compound is
707 selected for MS/MS fragmentation and then a fragment ion is monitored. These parent

mass > fragment ion mass transitions were 150>104 m/z for methionine and 192>104 m/z as well as 192>146 m/z for acetylated methionine. These transitions were detected using a triple quadrupole instrument. The collision energy for the cone and the cell were 15 V and 12 V respectively for the 192 to 104 and 192 to 146 transitions.

Isothermal titration calorimetry

ITC titrations were carried out on a PEAK ITC instrument (Malvern). Prior to the measurement, IF2, fMet-tRNA^{fMet} and acMet-tRNA^{fMet} were dialyzed to 50 mM MES pH 6.5, 100 mM KCl, 1 mM $MgCl_2$ and 0.5 mM TCEP. The samples were filtered and degassed for 10 min before being examined in the calorimeter and the titrations were performed at 35 °C. All the experiments consisted of injection of constant volumes of 2 µL of titrant into the cell (200 µL) with a stirring rate of 750 rpm. Nominal sample concentrations were between 2 µM and 5 µM in the cell and 40 µM to 50 µM in the syringe. Actual sample concentrations were determined after dialysis or buffer exchange by measurement of their absorption at 280 nm. All data were analyzed using the MicroCal Origin ITC 7.0

30S initiation complex formation

For 30S-IC assays ribosomes were isolated from WT *E. coli* DJ624Δ*ara* strain using sucrose gradient as described in ribosome purification section. 30S peak was pooled and exchanged to translation buffer using 100K Amicon centrifugation device (Millipore) to remove sucrose. IF1 and IF2 were purified as described in protein purification section. mRNA was produced using MEGAscript T7 transcription kit (Thermo Fisher Scientific) from synthetic dsDNA oligonucloetides *template-mRNA-F/R* provided in Supplementary table 2. tRNA^{fMet} was charged with [^{35}S]-Met and modified as described in

aminoacylation and acetylation methods sections, and then purified with mini quick spin RNA columns (Roche). Concentration of each tRNA was adjusted based on A260 and cpm. 20 µl reactions consisting of 0,6 µM 30S ribosomes, 2,4 µM IF1, 2,4 µM IF2, 1 µM mRNA, 0,6 µM [^{35}S]Met-tRNA^{fMet} and 1 mM GTP were carried out in translation buffer (10 mM HEPES pH 7.5, 70 mM NH_4Cl, 50mM KCl, 1 mM DTT). The complex formation was allowed for 10 min at 37°C, protein complexes were trapped on nitrocellulose filters. Filters were washed with 20 ml of translation buffer, air dried and trapped isotope was estimated in scintillation counter. Free [^{35}S]Met-tRNA^{fMet} passed through nitrocellulose filter was used as a blank. Each reaction was repeated 3-6 times.

Ribosome purification

Ribosomes from *E. coli* DJ624Δ*ara* strains were isolated and analyzed by sucrose gradient centrifugation as described[52] with some modifications. Bacterial strains were grown at 37°C in LB, induction of toxin and antitoxin was induced with 0.2 % arabinose and 0.5 mM IPTG respectfully at OD600nm = 0.2 and cultures were collected after 1 h of induction. 0,5 mg/ml of chloramphenicol was added 3 min before harvesting to fix the polysomes. Cells were resuspended in cold buffer 1 (20 mM HEPES-KOH pH 7.5, 4 mM β-mercaptoethanol, 6 mM $MgCl_2$, 30 mM NH_4Cl) and incubated on ice with 0.75 mg/ml lysozyme. Cells were frozen at -80°C overnight, thawed and centrifuged at 32000g for 30 min at 4°C. 10 A260 units were layered on the sucrose gradient (10-50%) prepared in buffer 2 (20 mM HEPES-KOH pH 7.5, 4 mM β-mercaptoethanol, 10 mM $MgCl_2$, 150 mM NH_4Cl) and centrifuged for 22h at 4°C at 24 000 rpm in SW41Ti rotor (Beckman). Gradient fractions (250 µl) were collected manually from the top to the bottom using glass capillary tube connected to a peristaltic pump at 4 rpm and UV absorbance was monitored at 260 nm. Gradient fractions of interest were extracted with

phenol:chloroform (1:1) mix and precipitated with ethanol. Resulting rRNA was dissolved in water and analyzed on 1% agarose gel stained with ethidium bromide.

Online references

47. Kitagawa, M. et al. Complete set of ORF clones of Escherichia coli ASKA library (a complete set of E. coli K-12 ORF archive): unique resources for biological research. *DNA Res* **12**, 291-9 (2005).
48. Buck, M., Connick, M. & Ames, B.N. Complete analysis of tRNA-modified nucleosides by high-performance liquid chromatography: the 29 modified nucleosides of Salmonella typhimurium and Escherichia coli tRNA. *Anal Biochem* **129**, 1-13 (1983).
49. Castro-Roa, D. & Zenkin, N. Methods for the assembly and analysis of in vitro transcription-coupled-to-translation systems. *Methods Mol Biol* **1276**, 81-99 (2015).
50. Janssen, B.D., Diner, E.J. & Hayes, C.S. Analysis of aminoacyl- and peptidyl-tRNAs by gel electrophoresis. *Methods Mol Biol* **905**, 291-309 (2012).
51. Walker, S.E. & Fredrick, K. Preparation and evaluation of acylated tRNAs. *Methods* **44**, 81-6 (2008).
52. Sobott, F., Hernandez, H., McCammon, M.G., Tito, M.A. & Robinson, C.V. A tandem mass spectrometer for improved transmission and analysis of large macromolecular assemblies. *Anal Chem* **74**, 1402-7 (2002).
53. Korber, P., Stahl, J.M., Nierhaus, K.H. & Bardwell, J.C. Hsp15: a ribosome-associated heat shock protein. *EMBO J* **19**, 741-8 (2000).
54. Perna, N.T. et al. Genome sequence of enterohaemorrhagic Escherichia coli O157:H7. *Nature* **409**, 529-33 (2001).
55. Guzman, L.M., Belin, D., Carson, M.J. & Beckwith, J. Tight regulation, modulation, and high-level expression by vectors containing the arabinose PBAD promoter. *J Bacteriol* **177**, 4121-30 (1995).
56. Brosius, J. & Holy, A. Regulation of ribosomal RNA promoters with a synthetic lac operator. *Proc Natl Acad Sci U S A* **81**, 6929-33 (1984).

57. Hallez, R. et al. New toxins homologous to ParE belonging to three-component toxin-antitoxin systems in Escherichia coli O157:H7. *Mol Microbiol* **76**, 719-32 (2010).
58. Christensen, S.K. et al. Overproduction of the Lon protease triggers inhibition of translation in Escherichia coli: involvement of the yefM-yoeB toxin-antitoxin system. *Mol Microbiol* **51**, 1705-17 (2004).
59. Dyda, F., Klein, D.C. & Hickman, A.B. GCN5-related N-acetyltransferases: a structural overview. *Annu Rev Biophys Biomol Struct* **29**, 81-103 (2000).
60. Grosjean, H., Keith, G. & Droogmans, L. Detection and quantification of modified nucleotides in RNA using thin-layer chromatography. *Methods Mol Biol* **265**, 357-91 (2004).

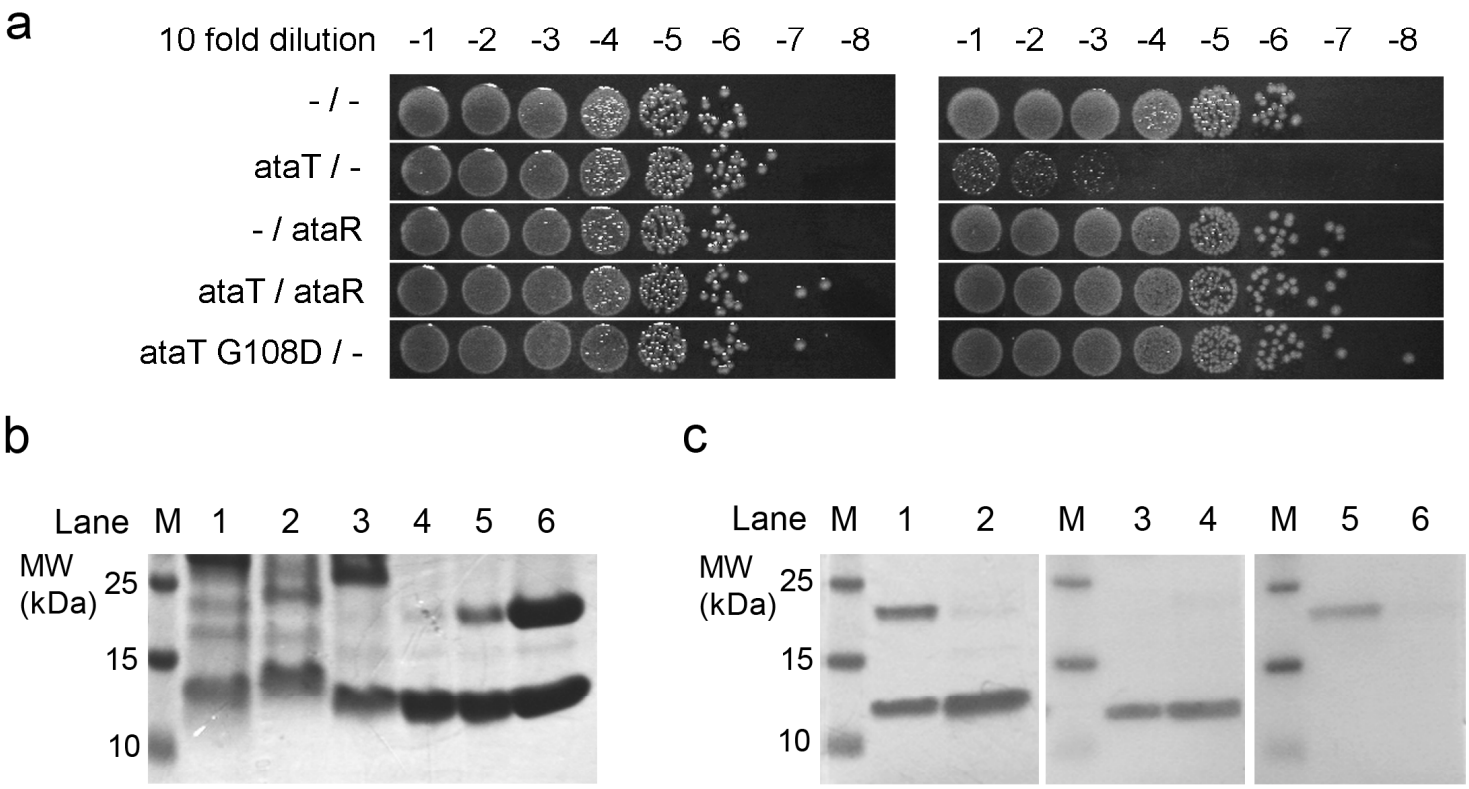
a
10 fold dilution
-1 -2 -3 -4 -5 -6 -7 -8
-1 -2 -3 -4 -5 -6 -7 -8
- / -
ataT / -
- / ataR
ataT / ataR
ataT G108D / -
b
Lane M 1 2 3 4 5 6
MW (kDa)
25
15
10
c
Lane M 1 2 M 3 4 M 5 6
MW (kDa)
25
15
10

a

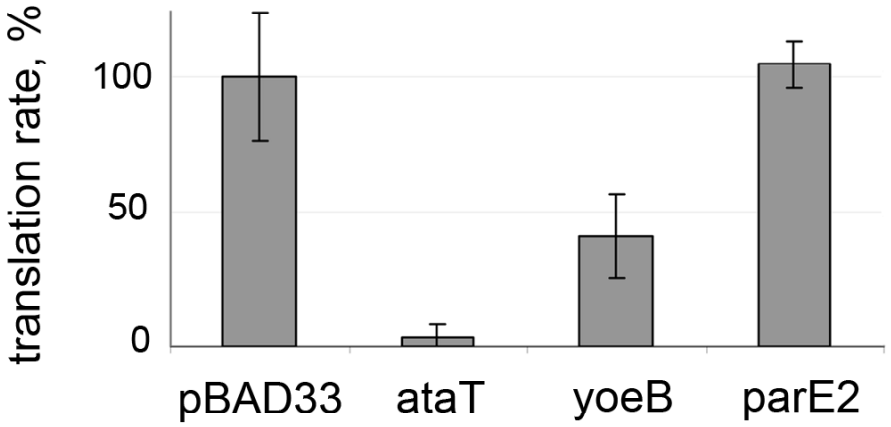
translation rate, %
100
50
0
pBAD33
ataT
yoeB
parE2

b

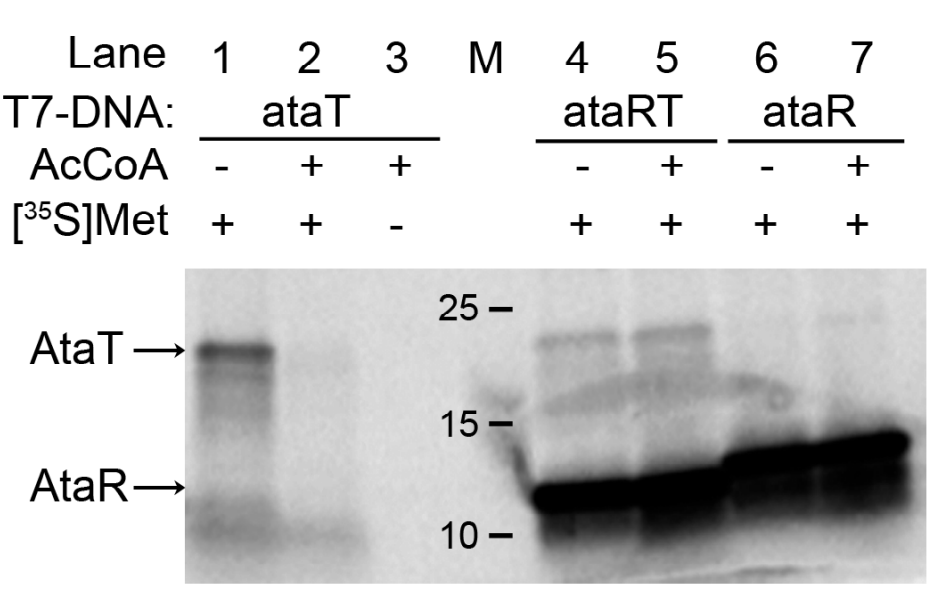
Lane 1 2 3 M 4 5 6 7
T7-DNA: ataT ataRT ataR
AcCoA - + + - + - +
[35S]Met + + - + + + +
AtaT
AtaR
25
15
10

c

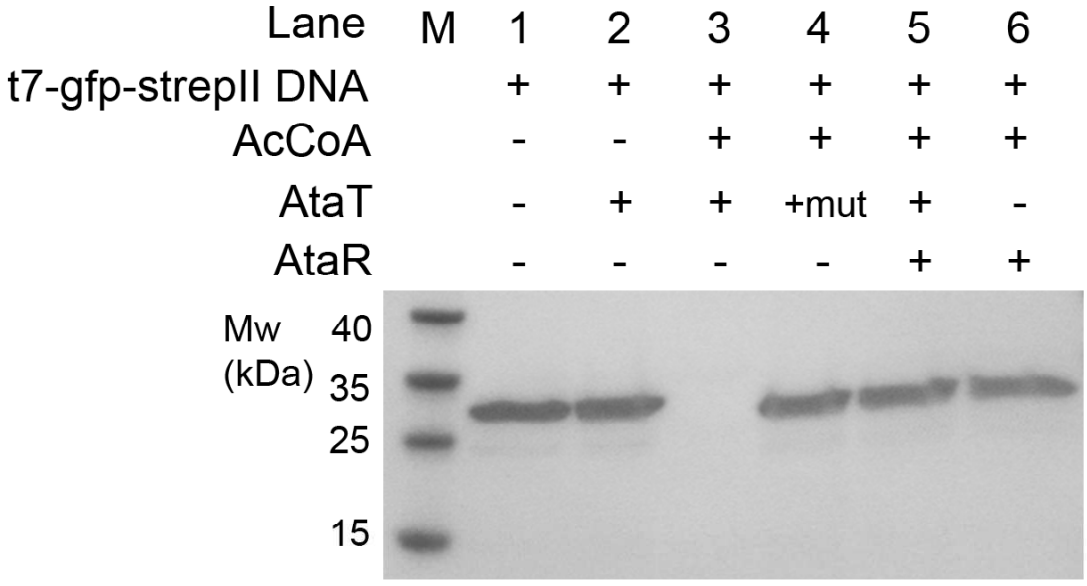
Lane M 1 2 3 4 5 6
t7-gfp-strepII DNA + + + + + +
AcCoA - - + + + +
AtaT - + + +mut + -
AtaR - - - - + +
Mw (kDa)
40
35
25
15

a

Lane	1	2	3	4	5	6	7	8	9
[^{14}C]AcCoA	+	+	+	+	+	+	+	+	+
AtaT	-	+	+	-	+	+	-	+	+
AtaR	-	-	+	-	-	+	-	-	+

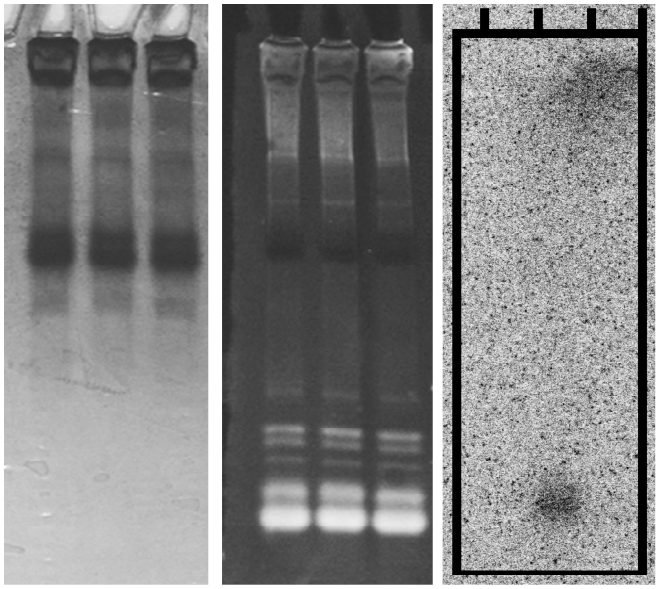

b

Lane	1	2	3	4	5
tRNA mix	+	+	+	+	+
[^{14}C]AcCoA	+	-	+	+	+
AtaT	-	+	+	+	+
AtaR	-	-	-	+	+*

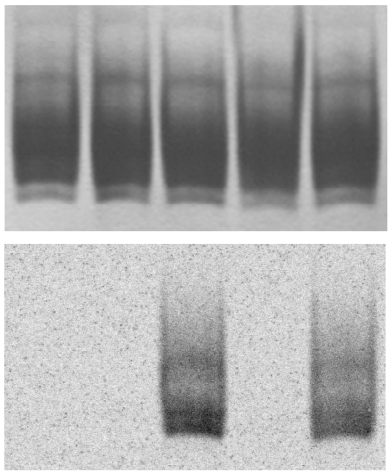

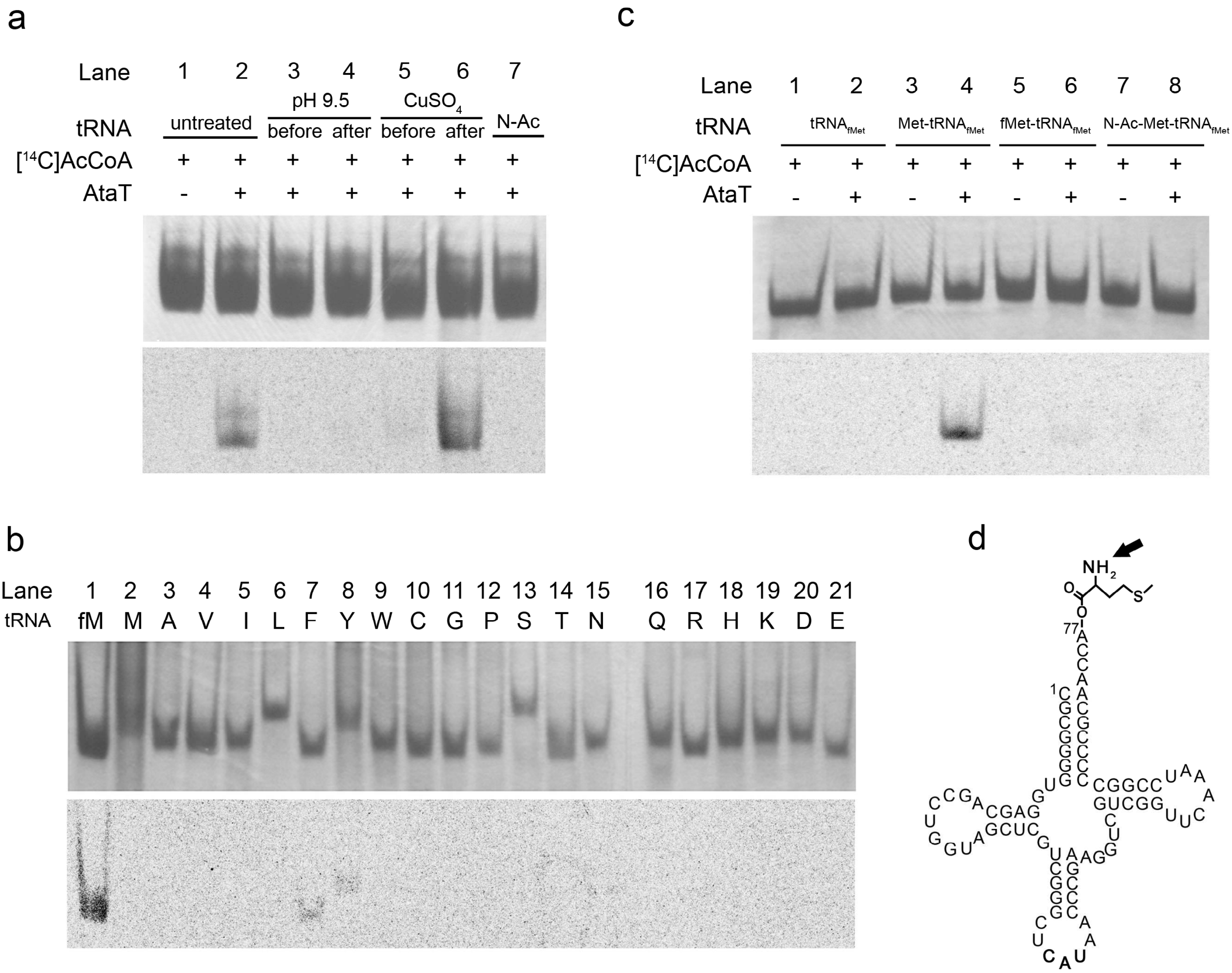
a
Lane 1 2 3 4 5 6 7
pH 9.5
CuSO4
tRNA untreated before after before after N-Ac
[14C]AcCoA + + + + + + +
AtaT - + + + + + +
c
Lane 1 2 3 4 5 6 7 8
tRNA tRNAfMet Met-tRNAfMet fMet-tRNAfMet N-Ac-Met-tRNAfMet
[14C]AcCoA + + + + + + + +
AtaT - + - + - + - +
b
Lane 1 2 3 4 5 6 7 8 9 10 11 12 13 14 15 16 17 18 19 20 21
tRNA fM M A V I L F Y W C G P S T N Q R H K D E
d
NH2
S
77
1

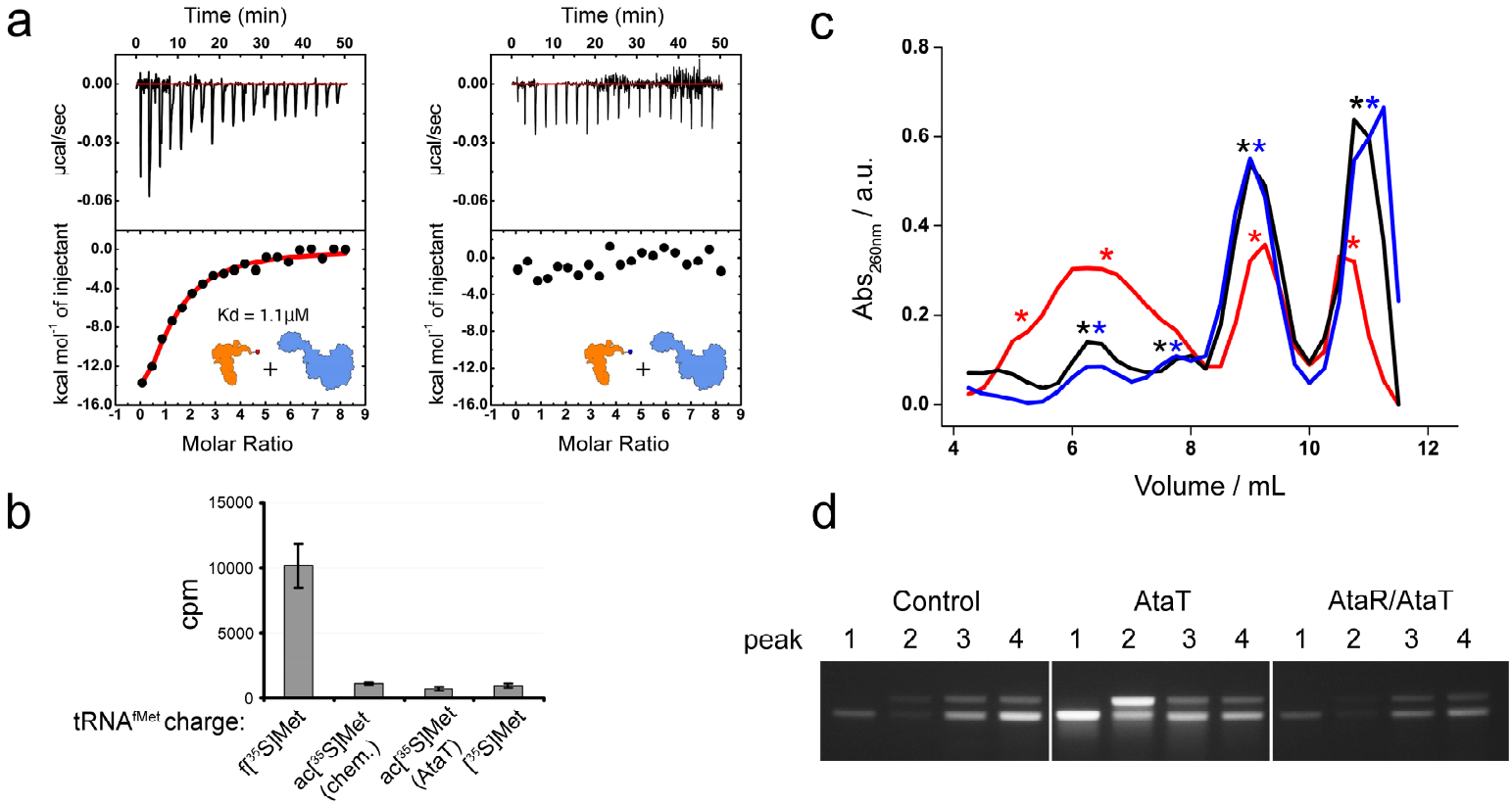
a
Time (min)
µcal/sec
kcal mol-1 of injectant
Kd = 1.1µM
Molar Ratio
b
cpm
tRNAfMet charge:
fI[35S]Met
acI[35S]Met (chem.)
acI[35S]Met (AtaT)
I[35S]Met
c
Abs260nm / a.u.
Volume / mL
d
Control
AtaT
AtaR/AtaT
peak

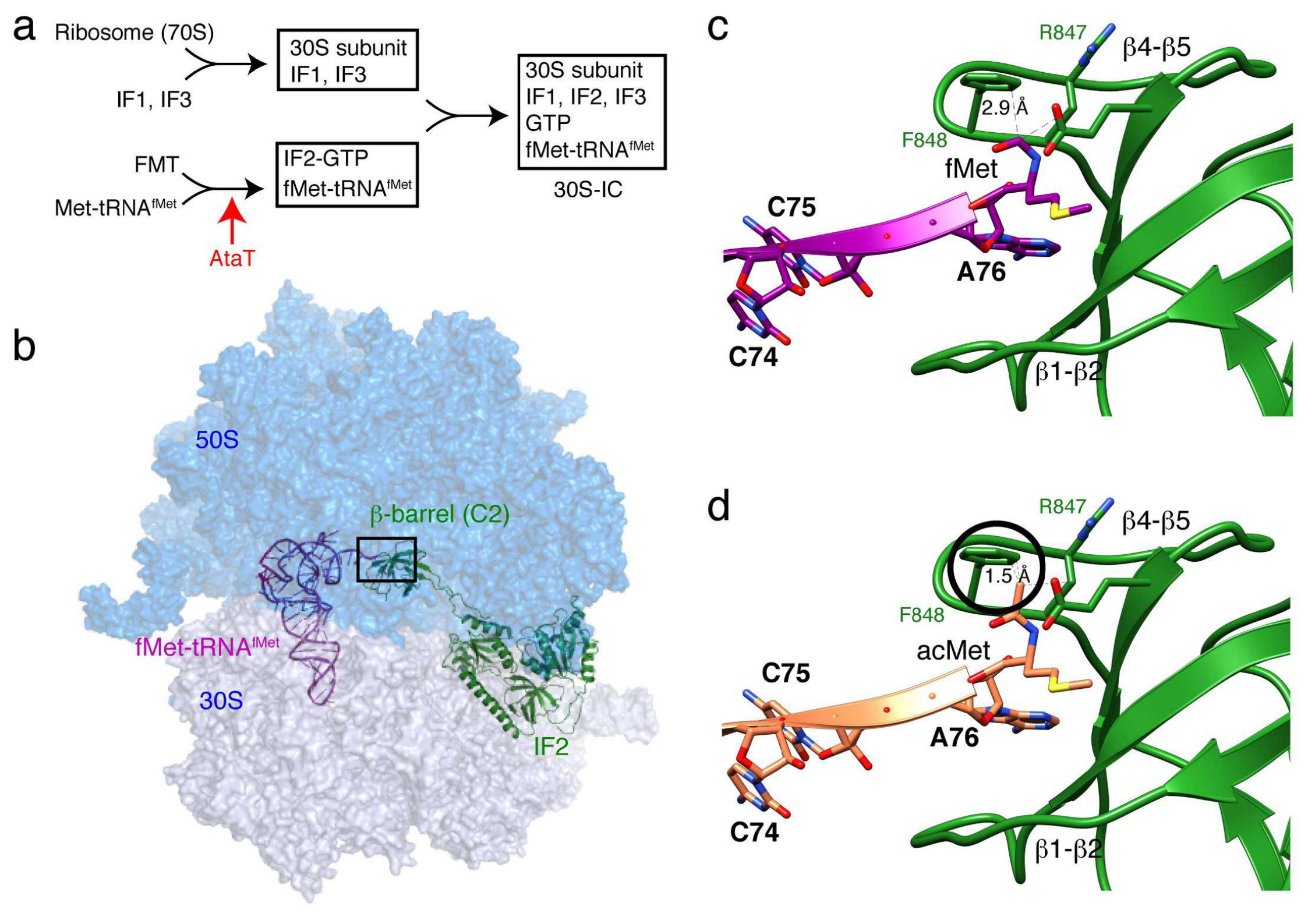
a
Ribosome (70S)
IF1, IF3
30S subunit
IF1, IF3
30S subunit
IF1, IF2, IF3
GTP
fMet-tRNA^fMet
30S-IC
FMT
Met-tRNA^fMet
IF2-GTP
fMet-tRNA^fMet
AtaT
b
50S
β-barrel (C2)
fMet-tRNA^fMet
30S
IF2
c
R847
β4-β5
2.9 Å
F848
fMet
C75
A76
C74
β1-β2
d
R847
β4-β5
1.5 Å
F848
acMet
C75
A76
C74
β1-β2

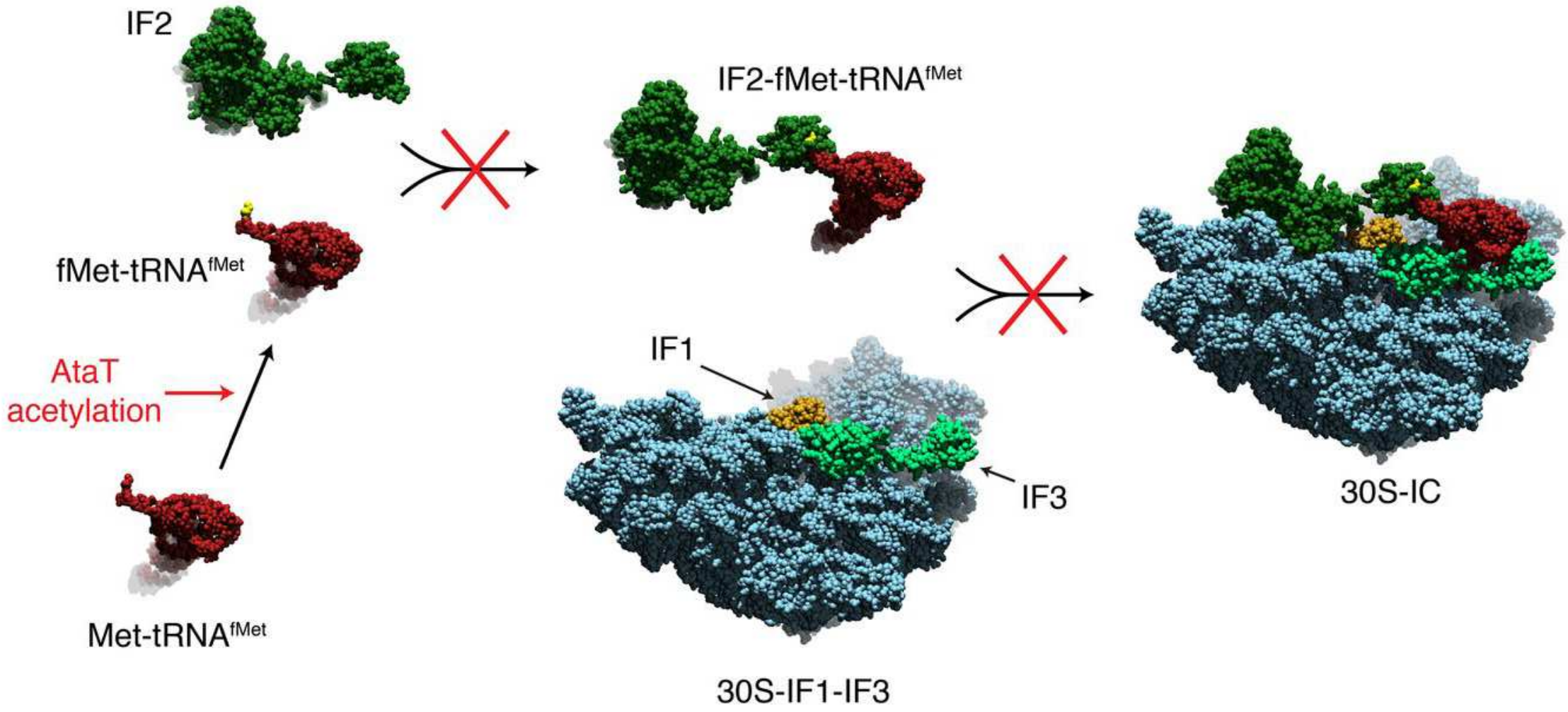
IF2
fMet-tRNA^fMet
AtaT
acetylation
Met-tRNA^fMet
IF2-fMet-tRNA^fMet
IF1
IF3
30S-IF1-IF3
30S-IC